White Rose Research Online

eprints@whiterose.ac.uk
https://eprints.whiterose.ac.uk
Universities of Leeds, Sheffield and York

Deposited via The University of Sheffield.

White Rose Research Online URL for this paper:
https://eprints.whiterose.ac.uk/id/eprint/103714/

Version: Accepted Version

Proceedings Paper:
Singh, R., Bai, Q., O'Farrell, T. et al. (2017) Demonstration of RF Digitising Concurrent Dual-Band Receiver for Carrier Aggregation over TV White Spaces. In: Vehicular Technology Conference (VTC-Fall), 2016 IEEE 84th. 2016 IEEE 84th Vehicular Technology Conference (VTC-Fall), 18-21 Sep 2016, Montreal, QC, Canada. IEEE. ISBN: 978-1-5090-1701-0.

https://doi.org/10.1109/VTCFall.2016.7880952

© 2016 IEEE. Personal use of this material is permitted. Permission from IEEE must be obtained for all other users, including reprinting/ republishing this material for advertising or promotional purposes, creating new collective works for resale or redistribution to servers or lists, or reuse of any copyrighted components of this work in other works.

Reuse
Items deposited in White Rose Research Online are protected by copyright, with all rights reserved unless indicated otherwise. They may be downloaded and/or printed for private study, or other acts as permitted by national copyright laws. The publisher or other rights holders may allow further reproduction and re-use of the full text version. This is indicated by the licence information on the White Rose Research Online record for the item.

Takedown
If you consider content in White Rose Research Online to be in breach of UK law, please notify us by emailing eprints@whiterose.ac.uk including the URL of the record and the reason for the withdrawal request.

UNIVERSITY OF LEEDS
University of Sheffield
UNIVERSITY of York

Demonstration of RF Digitising Concurrent Dual-Band Receiver for Carrier Aggregation over TV White Spaces

R. Singh, Q. Bai, T. O'Farrell, K. L. Ford, and R. J. Langley
Department of Electronic & Electrical Engineering,
The University of Sheffield, S1 3JD, UK
Email: {r.singh, q.bai, l.ford, t.ofarrell, r.j.langley}@sheffield.ac.uk

***Abstract*—In order to meet the high data rate, low latency and high energy efficiency requirements, the future radio units must utilise the frequency spectrum available at certain geographical location efficiently with a minimum amount of hardware. This requires frequency agility and concurrent multi-standard operation capabilities at the base and mobile terminals. To utilise the TV white spaces for mobile and wireless communication and enable their carrier aggregation with sub GHz LTE bands, this paper presents a single-chain, reconfigurable, RF digitising, dual-band receiver comprised of a tunable dual-band antenna, a reconfigurable digital down converter, a baseband processing unit and wideband LNA and ADC in the form of an oscilloscope. The presented dual-band receiver is tested through a hardware-in-the-loop test-bed which shows that up to 20 MHz aggregate bandwidths can be achieved. The receiver is able to provide equivalent error vector magnitude (EVM) performance across a wide range of frequencies avoiding any inter-band interference.**

I. Introduction

As the forthcoming mobile and wireless communication systems are being developed to avoid the foreseen capacity crunch, enabling dynamic spectrum usage is one of the key requirements to improve spectrum utilisation. Several studies [1][2][3] have found that, although most of the sub 6 GHz spectrum has been assigned for various communication technologies, the usage of this spectrum varies geographically leading to underutilisation of spectrum. Carrier aggregation (CA) [4] and cognitive radio (CR) [5] are amongst the key enabling techniques for the efficient use of spectrum available at certain geographical location. Therefore, frequency agility and concurrent multi-band operation are highly important for the future radio devices.

In addition, the future communication networks are expected to be highly heterogeneous, working concurrently over different types of current and future radio access technologies (RATs), and various communication standards, to meet the foreseen demands of high data rate, lower latencies and higher energy efficiency [6]. Therefore, the base stations (BSs) and the user equipments (UEs) must be equipped with not only the existing but also the forthcoming mobile and wireless communication radio units, increasing the total number of transceiver chains. This will increases the overall system size and cost. Therefore, the future radio terminals must also minimise the number of transceiver chains, while allowing concurrent multi-band, multi-standard transmissions.

Digitising at RF directly can lead to reconfigurable yet small, power efficient and cost effective radio front ends [7]. Based on direct RF digitisation, a frequency agile and concurrent multi-band single-chain radio receiver may resemble Fig.1, which comprises a multi-band tunable analogue front-end, a multi-band reconfigurable ADC and digital down-converter (DDC), and a baseband processing unit. In such receivers, the DDC will frequency translate a digitised multi-band RF signal to multiple narrowband or single wide-band baseband signal. In recent years, research in multi-band tunable antennas [8], LNAs [9], and reconfigurable ADCs [10] has started, however, these components are not commercially available yet.

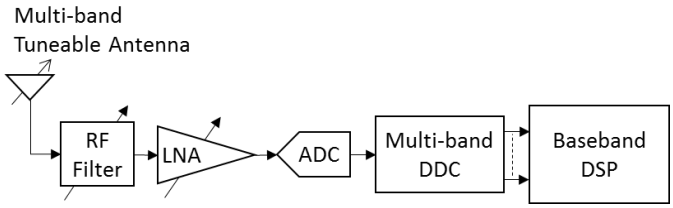

Fig. 1. Block diagram of a direct RF digitising receiver.

In this paper, a direct RF digitising concurrent dual-band receiver with capabilities to operate from 560 MHz to 1.1 GHz, focusing on CA between the TV white spaces (TVWSs) and LTE bands is presented, and its performance is evaluated through a hardware-in-the-loop test-bed. The receiver utilises a tunable dual-band antenna, a DSO acting as a wideband RF digitiser, a reconfigurable dual-band DDC and a baseband processing unit.

The EVM results for various CA scenarios between the LTE and digital terrestrial television (DTT) bands are evaluated using two concurrent but independent single carrier (SC) transmissions. The results show that the narrowband tunable antenna and digital filtering provide significant isolation between the LTE and DTT bands and minimise inter-band interference. The results also show that the system performance is almost identical across the frequency bands of interest.

II. Test-bed Description

This section details the test-bed set-up at the transmitter (Tx) and receiver (Rx) ends for the EVM evaluation of two concurrent transmissions utilising TVWS and LTE bands.

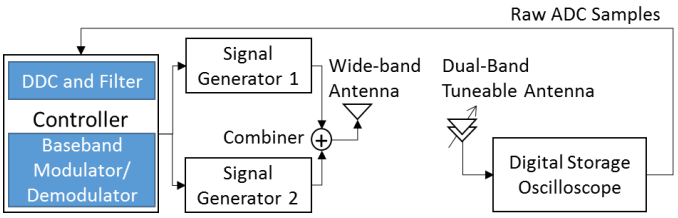

Fig. 2. Block diagram of the RF digitising dual-band test-bed.

A. Transmitter

A system level block diagram of the test-bed is shown in Fig. 2. At the heart of the hardware-in-the-loop test-bed is the controller (PXIe-8135) [11], which is essentially a PC running LabVIEW and MATLAB software packages. The baseband signal processing takes place in the controller, where two different baseband I/Q signals are generated in LabVIEW and sent to the dedicated reconfigurable RF signal generators (PXIe-5793) [12] operating at two distinct RF frequencies. The RF output of the signal generators is combined by ZAPD-2-272-S+ [13] and the combined signal is transmitted through a wideband antenna (UHALP-9108 A) [14].

B. Receiver

The RF digitising receiver comprises a tunable dual-band antenna, a digital storage oscilloscope (DSO) [15] acting as an RF digitiser, a reconfigurable dual-channel digital down-converter (DDC) and baseband processors.

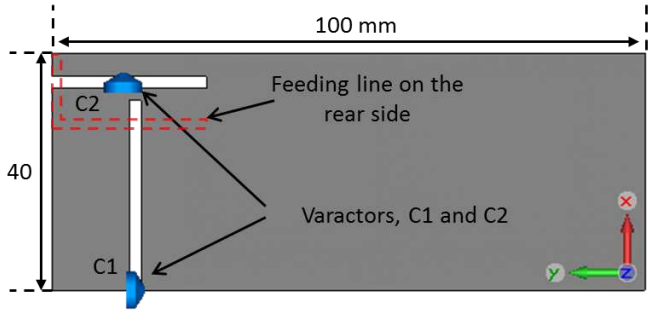

Fig. 3. Geometry of tunable dual-band antenna.

Tuneable Dual-Band Antenna: The antenna on the Rx side is designed to support two bands simultaneously with each band independently tunable specifically covering the DTT and sub 1 GHz LTE bands. As shown in Fig. 3, this antenna consists of two slots which are placed perpendicularly to each other on the ground plane of the UE's main board and fed by a 50Ω stripline on the other side of the PCB. The overall dimensions of the PCB are 100 mm × 40 mm × 1.6 mm, and the actual antenna size is only 26 mm × 36 mm. Two varactors

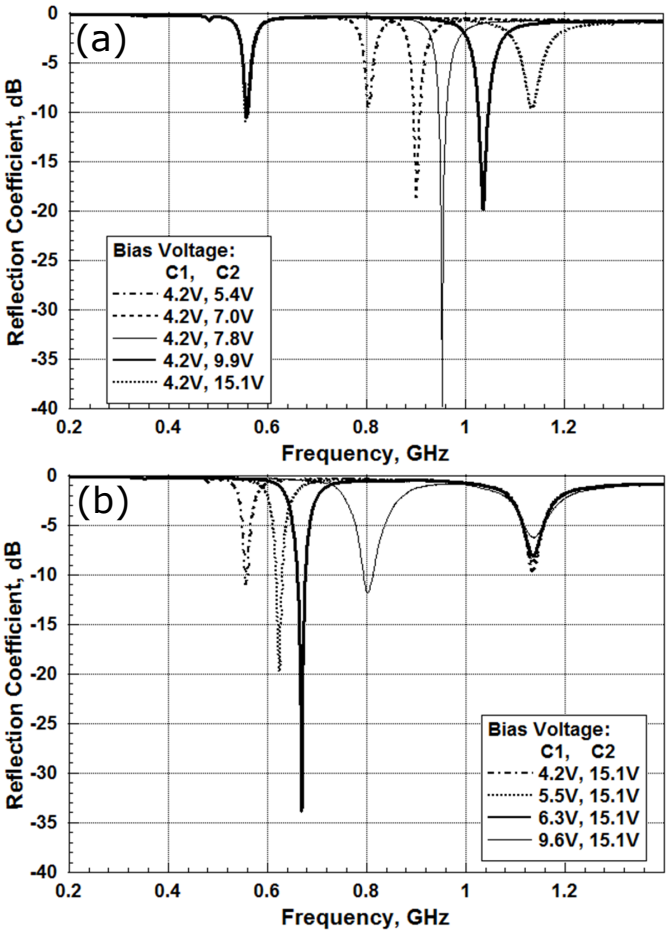

Fig. 4. Measured antenna reflection coefficient with varying bias voltages of C1 and C2: (a) Higher band tuning; (b) Lower band tuning.

(BB833) [16] with bias networks are used to tune these two slots, consequently, two individual tunable frequency bands.

The measured antenna reflection coefficients are shown in Fig. 4, from where we can see that the antenna lower band (Fig. 4(b)) -6 dB tuning range covers from 560 MHz to 800 MHz, and the higher band (Fig. 4(a)) can be tuned from 800 MHz to 1.1 GHz, which fully covers the desired frequency range of 0.6 ∼ 1 GHz. It is also noticed that tuning one band will not affect the resonant frequency of the other band, which is very important for this dual-band independently tunable antenna design. The measured antenna gain is -1.8 dBi at 650 MHz, -2.4 dBi at 800 MHz and -3.9 dBi at 1 GHz.

Digital Down-Conversion and Baseband DSP: The mixed RF signal detected by the dual-band antenna is directly digitised by the DSO at a sampling rate of 5 GSPS in the receiver chain. The controller acquires the digitised signal (or the raw ADC samples) from the DSO through a direct Ethernet link, where the DDC and baseband demodulation takes place, respectively.

The block diagram of a dual-channel DDC is shown in Fig. 5 along with baseband processing units. DDC provides frequency conversion and decimation filtering of desired bands

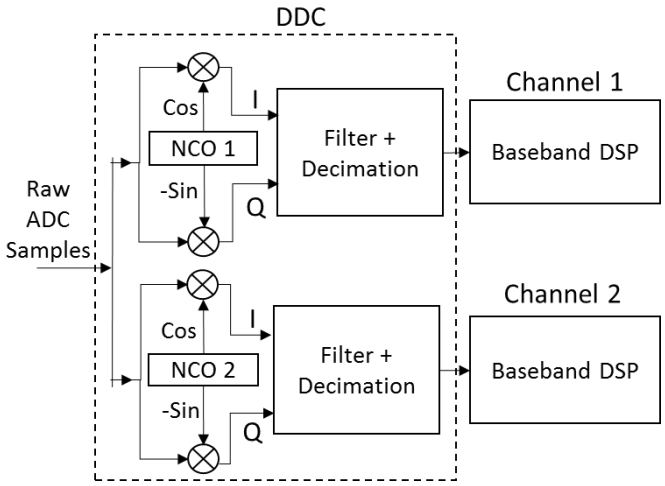

Fig. 5. Block diagram of a dual-channel reconfigurable digital receiver.

before the baseband demodulation takes place. The real digital RF signal in the form of ADC samples is mixed with complex outputs of two different digital synthesisers know as numerically controllable oscillators (NCO). The DDC was implemented as a direct (or a homodyne) converter. Therefore, the centre frequency of the two NCOs was set equal to the carrier frequency of the two signals generated at the Tx. This provides the baseband I/Q samples for the two channels.

The baseband signal is then passed through a cascaded integrated comb (CIC) decimation filter, which provides image and out-of-band rejection, as well as sample rate reduction to desired level. In this work, the DDC was implemented using MATLAB DSP function, where the NCO centre frequencies, the CIC stopband frequency and attenuation, and decimation factors where configured according to the bandwidth and carrier frequency of the incoming signals. The filtered, decimated baseband signals are then processed in LabVIEW, where the timing, carrier and phase offsets are removed through the use of a synchronisation sequence and by locking to the carrier signal. Then matched filtering is performed before the *rms* EVM is estimated through equation (1) [17], where N is the number of samples received, I and Q are the ideal in-phase and quadrature levels, and $\tilde{I}$ and $\tilde{Q}$ are the received in-phase and quadrature values.

$$\text{EVM}_{rms} = \sqrt{\frac{\frac{1}{N}\sum_{i=1}^{N}(I_i - \tilde{I}_i)^2 + (Q_i - \tilde{Q}_i)^2}{\frac{1}{N}\sum_{i=1}^{N}(I_i^2 + Q_i^2)}} \times 100 \quad (1)$$

III. Experimentation, Results and Analysis

A. Experimental Set-up

Although the tunable dual-band antenna can be operated from 560 MHz to 1.1 GHz, which can cover all the DTT and sub GHz mobile bands, in order to avoid any interference to or from the operating DTT and LTE bands, only unoccupied LTE and DTT bands were used during the experimentation. The 8 MHz wide TVWSs present in the Sheffield (UK) region were used, which correspond to DTT bands 43, 46, 49, 50 and 57, with actual transmission bandwidth of 6 MHz due to guard band requirements. The adjacent DDT bands 49 and 50 were used as a single transmission channel. Each of these unoccupied DTT bands were aggregated with a 10 MHz wide transmission utilising the unoccupied part of LTE band 20, giving an aggregated bandwidth of 16-20 MHz. The band span and corresponding centre frequencies (f_c) of these bands are shown in Table I.

TABLE I
THE TVWSS (DTT BANDS) AND LTE BANDS USED IN EXPERIMENTATION.

Band	Span (MHz)	f_c (MHz)
DTT 43	646 - 654	650
DTT 46	670 - 678	674
DTT 49+50	694 - 710	702
DTT 57	758 - 766	762
LTE 20[1]	791 - 801	796

In order to characterise the concurrent dual-band receiver, single carrier (SC) QPSK and 16-QAM modulation schemes with root raise cosine filtering at a roll-off (β) of 0.5 were used and the *rms* EVM for each data-link was evaluated. The experimentation was carried out in a typical working environment, where the Tx and Rx were placed at a height of 1.1m with a separation of 2m.

B. Results and Discussion

Table II shows the different combinations of the DTT and LTE bands used with different types of baseband modulation techniques to examine the performance of the single-chain dual-band receiver. Fig. 6 shows the EVM_{rms} vs received power (dBm) results of the combinations shown in Table II. Theses results show that for the same modulation format, the dual-band receiver provides almost identical EVM_{rms} performance across different combinations of bands, e.g. in combinations (a), (b), (c), (d) and (e) with QPSK modulation and in combination (e) and (f) for 16-QAM modulation.

TABLE II
EXAMINED COMBINATIONS OF DTT AND LTE BANDS FOR CA.

Combination	Combined Bands	Used Modulation	Aggregate Bandwidth (MHz)
(a)	DTT 43 & LTE 20	Both QPSK	16
(b)	DTT 46 & LTE 20	Both QPSK	16
(c)	DTT 57 & LTE 20	Both QPSK	16
(d)	DTT 49+50 & LTE 20	Both QPSK	20
(e)	DTT 49+50 & LTE 20	16-QAM & QPSK	20
(f)	DTT 49+50 & LTE 20	Both 16-QAM	20

[1]Only 791-801 MHz part of this band was used.

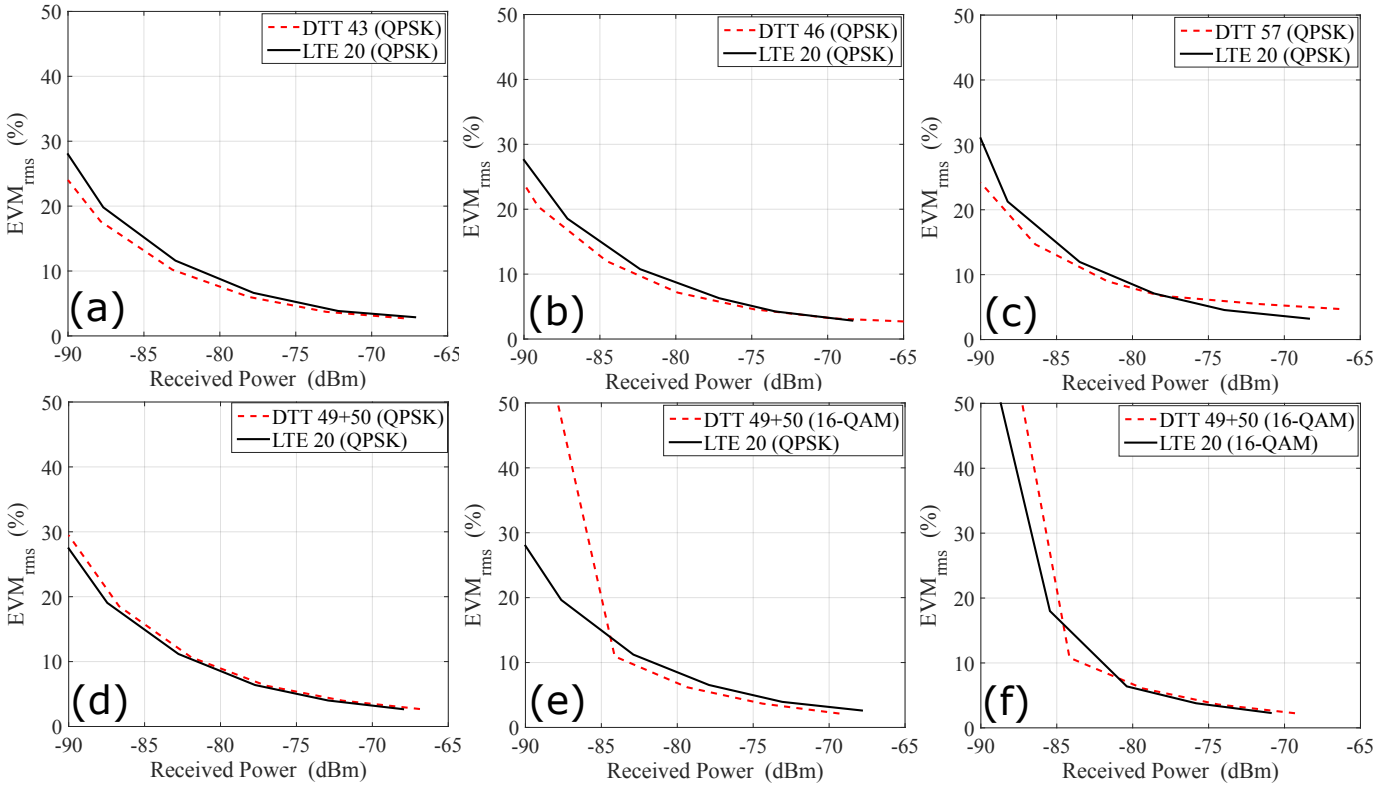

Fig. 6. EVM$_{rms}$ (%) of QPSK and 16-QAM based single carrier signals over carrier aggregated TVWS and LTE bands received through RF digitising concurrent dual-band receiver. Results from (a) to (f) correspond to combinations listed in Table II.

The results of combinations E and F also indicate the performance difference between a QPSK and a 16-QAM link. The EVM$_{rms}$ of 16-QAM transmissions increase sharply as the received power drops below -84 dBm. This is due to the higher SNR requirements of a 16-QAM transmission in comparison to a QPSK transmission.

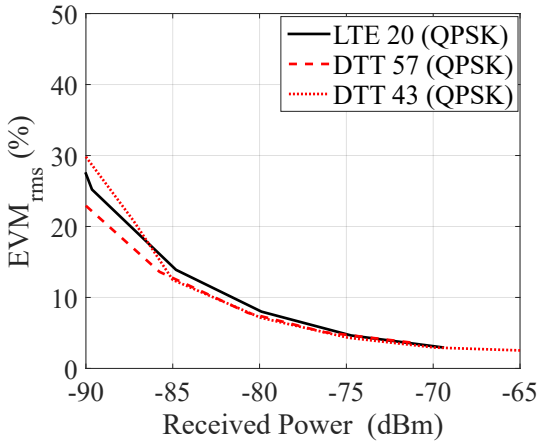

Fig. 7. EVM$_{rms}$ (%) of QPSK based single carrier signals over DTT and LTE bands without CA.

In order to investigate the inter-band interference between the LTE and DTT bands, experiments without the use of CA were also carried out, where the EVM$_{rms}$ of QPSK based SC transmissions over LTE and DTT bands was evaluated separately. In this investigation, the bands with a small gap i.e. the LTE 20 and DTT 57, and the bands with a large gap i.e. LTE 20 and DTT 43 were used. The result of these experiments are shown in Fig. 7, which when compared to the results in Fig. 6 show that the EVM$_{rms}$ performance of the system remains approximately the same irrespective of the use of CA. This shows that the analogue filtering at the dual-band tunable antenna and the digital filtering through the CIC decimation filter is sufficient to avoid any harmful interference between the LTE and DTT bands. However, further care must be taken at the transmit side, while working with multi-carrier signal, where the high PAPR can lead to out-of-band radiation [18]. The development of techniques such as symbol erasure [19][20] to mitigate the LTE DTT coexistence interference is also important.

Overall, this demonstration shows how reconfigurable single-chain multi-band receivers can be realised through a multi-band antenna and a reconfigurable DDC. Although the DDC in this work was implemented on MATLAB, however, it can also be implemented on an FPGA for real-time transmissions. The RF digitising DSO acted as a wide-band LNA and ADC in this work. However, a final receiver design with multi-band LNA and multi-band ADC capabilities can further increase the overall receiver sensitivity. This is a topic of further research for the authors.

IV. Conclusion

This paper presents a reconfigurable RF digitising concurrent dual-band receiver, specifically designed to utilise the TV white spaces for CA with sub GHz LTE bands. The receiver comprises a tunable dual-band antenna, a wideband LNA and ADC in the form of an oscilloscope, a dual-band DDC and a baseband processing unit. The EVM performances of QPSK and 16-QAM based concurrent transmissions over the unoccupied DTT and LTE bands are evaluated, which shows that up to 20 MHz of aggregate bandwidth can be achieved. The results also show that the system EVM performance remains equivalent for various CA combinations between the LTE and DTT bands. The analogue filtering at the receiver antenna and the digital filtering in the DDC provide good isolation between the two simultaneously received signals to avoid any harmful interference.

As a part of future work, the authors are working on the implementation of representative mobile communication standards in the test-bed such that the overall throughputs increments with concurrent transmissions can be estimated.

V. Acknowledgement

This work was carried out in FARAD project, funded by the UK government under the EPSRC grant EP/M013723/1.

References

[1] V. Valenta, R. Maršálek, G. Baudoin, M. Villegas, M. Suarez, and F. Robert, "Survey on spectrum utilization in Europe: Measurements, analyses and observations," in *Cognitive Radio Oriented Wireless Networks & Communications (CROWNCOM), 2010 Proceedings of the Fifth International Conference on*. IEEE, 2010, pp. 1–5.

[2] I. F. Akyildiz, W.-Y. Lee, M. C. Vuran, and S. Mohanty, "NeXt generation/dynamic spectrum access/cognitive radio wireless networks: a survey," *Computer networks*, vol. 50, no. 13, pp. 2127–2159, 2006.

[3] ——, "A survey on spectrum management in cognitive radio networks," *Communications Magazine, IEEE*, vol. 46, no. 4, pp. 40–48, 2008.

[4] Evolved Universal Terrestrial Radio Access, "Further advancements for E-UTRA physical layer aspects," 3GPP TR 36.814, Tech. Rep., 2010.

[5] P. Pawelczak, K. Nolan, L. Doyle, S. W. Oh, and D. Cabric, "Cognitive radio: Ten years of experimentation and development," *Communications Magazine, IEEE*, vol. 49, no. 3, pp. 90–100, 2011.

[6] NGMN Alliance, "5G white paper," *Next Generation Mobile Networks, White paper*, 2015.

[7] Texas Instruments, "RF Sampling and GSPS ADCs: Breakthrough ADCs Revolutionize Radio Architectures," 2012. [Online]. Available: http://www.ti.com/lit/sg/snwt001/snwt001.pdf

[8] B. Avser and G. M. Rebeiz, "Tunable Dual-Band Antennas for 0.7–1.1-GHz and 1.7–2.3-GHz Carrier Aggregation Systems," *Antennas and Propagation, IEEE Transactions on*, vol. 63, no. 4, pp. 1498–1504, 2015.

[9] M. T. Mustaffa, A. Zayegh, and T. Z. A. Zulkifli, "A reconfigurable LNA for multi-standard receiver using 0.18 μm CMOS technology," in *Research and Development (SCOReD), 2009 IEEE Student Conference on*. IEEE, 2009, pp. 238–241.

[10] J. Marttila, M. Allén, and M. Valkama, "Frequency-agile multiband quadrature sigma-delta modulator for cognitive radio: Analysis, design and digital post-processing," *Selected Areas in Communications, IEEE Journal on*, vol. 31, no. 11, pp. 2222–2236, 2013.

[11] National Instruments, "Embedded Controller, PXIe-8135." [Online]. Available: http://www.ni.com/datasheet/pdf/en/ds-403

[12] ——, "Embedded Signal Generator, PXIe-5793." [Online]. Available: http://www.ni.com/pdf/manuals/373949b.pdf

[13] Mini Circuits, "Power Combiner/Splitter, ZAPD-2-272-S+." [Online]. Available: http://194.75.38.69/pdfs/ZAPD-2-272+.pdf

[14] Schwarzbeck, "Log-Periodic Antenna, UHALP-9108 A." [Online]. Available: http://www.schwarzbeck.de/en/antennas/logarithmic-periodic-broadband-antennas/standard-lpda/205-uhalp-9108-a.html

[15] LeCroy, "WaveSurfer MXs-A Oscilloscopes 200 MHz 1 GHz, 104MXs-A." [Online]. Available: http://teledynelecroy.com/japan/pdf/cata/wsxs-msxs-a-ds-12oct10-pdf.pdf

[16] Infineon, "Silicon Tuning Diodes." [Online]. Available: http://www.farnell.com/datasheets/1835975.pdf

[17] "IEEE Standard for Local and Metropolitan Area Networks Part 16: Air Interface for Fixed Broadband Wireless Access Systems," *IEEE Std 802.16-2004 (Revision of IEEE Std 802.16-2001)*, pp. 01–857, 2004.

[18] G. Fettweis, M. Krondorf, and S. Bittner, "GFDM-generalized frequency division multiplexing," in *Vehicular Technology Conference, 2009. VTC Spring 2009. IEEE 69th*. IEEE, 2009, pp. 1–4.

[19] L. Aguado, K. Wong, and T. O'Farrell, "Coexistence issues for 2.4 GHz OFDM WLANS," in *3G Mobile Communication Technologies, 2002. Third International Conference on (Conf. Publ. No. 489)*. IET, 2002, pp. 400–404.

[20] K. Wong and T. O'Farrell, "Coverage of 802.11 g WLANs in the presence of Bluetooth interference," in *Personal, Indoor and Mobile Radio Communications, 2003. PIMRC 2003. 14th IEEE Proceedings on*, vol. 3. IEEE, 2003, pp. 2027–2031.